ACS APPLIED MATERIALS & INTERFACES

Research Article

www.acsami.org

Tailored Surface Structure of $LiFePO_4$/C Nanofibers by Phosphidation and Their Electrochemical Superiority for Lithium Rechargeable Batteries

Yoon Cheol Lee,[†,‡] Dong-Wook Han,[§,‡] Mihui Park,[†] Mi Ru Jo,[†] Seung Ho Kang,[†] Ju Kyung Lee,[#] and Yong-Mook Kang*[,†]

[†]Department of Energy and Materials Engineering, Dongguk University-Seoul, Seoul, 100-715, Republic of Korea

[§]Department of Materials Science and Engineering, Korea Advanced Institute of Science and Technology, Yuseong, Daejeon, 305-340, Republic of Korea

[#]School of Energy and Chemical Engineering, Ulsan National Institute of Science and Technology, Banyeon-ri, Eonyang-eup, Ulju-gun, Ulsan, 689-798, Republic of Korea

Supporting Information

ABSTRACT: We offer a brand new strategy for enhancing Li ion transport at the surface of $LiFePO_4$/C nanofibers through noble Li ion conducting pathways built along reduced carbon webs by phosphorus. Pristine $LiFePO_4$/C nanofibers composed of 1-dimensional (1D) $LiFePO_4$ nanofibers with thick carbon coating layers on the surfaces of the nanofibers were prepared by the electrospinning technique. These dense and thick carbon layers prevented not only electrolyte penetration into the inner $LiFePO_4$ nanofibers but also facile Li ion transport at the electrode/electrolyte interface. In contrast, the existing strong interactions between the carbon and oxygen atoms on the surface of the pristine $LiFePO_4$/C nanofibers were weakened or partly broken by the adhesion of phosphorus, thereby improving Li ion migration through the thick carbon layers on the surfaces of the $LiFePO_4$ nanofibers. As a result, the phosphidated $LiFePO_4$/C nanofibers have a higher initial discharge capacity and a greatly improved rate capability when compared with pristine $LiFePO_4$/C nanofibers. Our findings of high Li ion transport induced by phosphidation can be widely applied to other carbon-coated electrode materials.

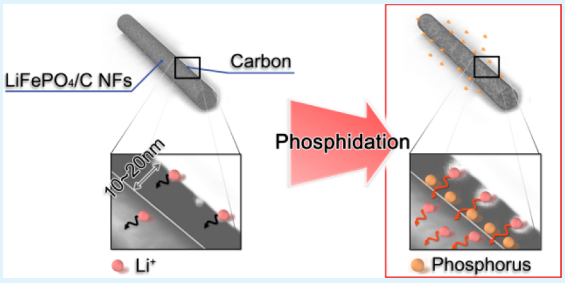

KEYWORDS: *$LiFePO_4$, lithium rechargeable battery, olivine structure, nanofiber, phosphidation*

INTRODUCTION

Emerging future technologies, including electric vehicles, uninterruptible power supplies, and smart grids, require the development of cathode materials for low-cost lithium ion batteries with excellent thermal stability and a long cycle life.[1−3] Olivine-structured $LiFePO_4$ is considered a particularly attractive cathode material to satisfy these requirements because it has numerous advantages, such as a high theoretical capacity (170 mA h g^{-1}), a moderate redox potential (Fe^{2+}/Fe^{3+}, 3.45 V), excellent cycling performance, abundance of natural iron resources, and environmental benignity.[4−8] However, practical applications of $LiFePO_4$ have been limited by its inherently poor kinetic properties that are caused by low electronic and ionic transfer ($\sigma_e = 10^{-1}$ S cm^{-1}, $D_{Li+} = 10^{-14}$ cm^2 s^{-1} at room temperature) in the lattice structure of $LiFePO_4$.[9−12] The kinetic properties of $LiFePO_4$ have been substantially improved by particle size reduction to the nanoscale[13−17] and/or carbon coatings.[18−21]

$LiFePO_4$/C composites composed of 1-dimensional (1D) $LiFePO_4$ nanofibers and conductive carbon have attracted much attention because of large reaction area on the surface of $LiFePO_4$ nanofibers, short Li ion diffusion length into the nanofibers, and the formation of facile electronic pathways through carbon webs, which enhance both ionic and electrical conductivities in the lattice structure of $LiFePO_4$.[22−24] A variety of efforts has been undertaken to generate $LiFePO_4$/C nanofibers, including sol−gel, hydrothermal, and electrospinning processes. We found here that the concentration of carbon exerts a significant influence on the electrochemical performance of $LiFePO_4$/C nanofibers. In particular, if the carbon content in $LiFePO_4$/C nanofibers exceeds an optimum value, Li ion migration through interfaces between $LiFePO_4$ nanofibers and an electrolyte is hindered by thick carbon layers that form on the surface of the nanofibers.[25−27]

In general, the electrospinning technique has been considered as one of the most promising approaches to control the diameter and the aspect ratio of $LiFePO_4$ nanofibers with high uniformity, but excess carbon has also negatively affected

Received: March 25, 2014
Accepted: May 2, 2014
Published: May 2, 2014

   dx.doi.org/10.1021/am5018122 | ACS Appl. Mater. Interfaces 2014, 6, 9435−9441

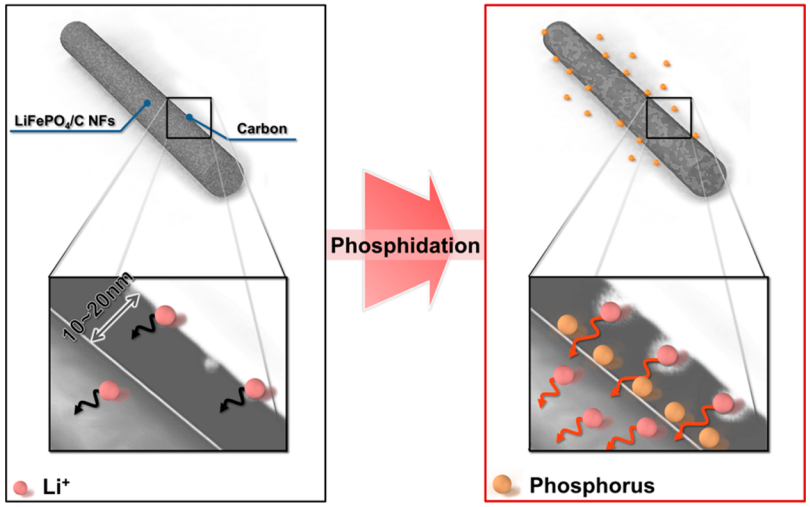

Figure 1. Schematic illustration of pristine and phosphidated $LiFePO_4$/C nanofibers.

the electrochemical performance of electrospun $LiFePO_4$ nanofibers.[28,29] To form a viscoelastic jet for electrospinning, a large amount of an organic polymer (PVP, PAN, etc.) should be uniformly dispersed in a mixed solution of $LiFePO_4$ precursors. In addition, when crystalline $LiFePO_4$ nanofibers are formed at high temperatures (≥550 °C), the organic polymers involved in the $LiFePO_4$ precursor mixture are thermally decomposed and then converted in situ to conductive carbon. Unfortunately, due to the lack of carbon combustion reactions during the synthesis of $LiFePO_4$/C nanofibers under an inert (N_2, Ar) or a reductive (H_2/N_2, H_2/Ar) atmosphere, thick carbon layers are inevitably coated on the surface of $LiFePO_4$ nanofibers. According to a recent study by Toprakci et al.,[30] electrospun $LiFePO_4$/C nanofibers with a high carbon content (22.5 wt %), as well as dense and thick carbon coating layers (15 nm), showed a lower initial discharge capacity, a higher polarization voltage, and inferior cycling performance compared to relatively low carbon containing nanofibers (17.0 and 14.3 wt %). They stated that the thick carbon coating layers that formed on the surface of the $LiFePO_4$ nanofibers could prevent not only electrolyte penetration into inner active material but also facile Li ion transport at the electrode/electrolyte interface.

In this study, the electrochemical performance of the $LiFePO_4$/C nanofibers was improved through the thermal decomposition of trioctylphosphine (TOP), which resulted in the formation of noble Li ion-conducting pathways along the reduced carbon webs by phosphorus (Figure 1). The resulting phosphidated $LiFePO_4$/C nanofibers have a higher initial discharge capacity and a greatly improved rate capability when compared to pristine $LiFePO_4$/C nanofibers. The electrical conductivity of the $LiFePO_4$ nanofibers can be readily enhanced to a practical level by an appropriate amount of carbon coating. Therefore, the critical focus must now be on improving the ionic conductivity of Li, especially at the surface of nanofibers on which thick carbon-coating layers are formed. In carbonaceous materials, including amorphous carbon, carbon nanotubes, and graphene, their crystallinity and the degree of the carbon network decreased and the number of inner defect sites increased through phosphorus incorporation.[31−35] Hence, phosphidated carbons have been utilized as the catalysts for oxygen reduction in fuel cells. Our present experiment confirmed that the existing strong interactions between carbon and oxygen atoms on the surface of $LiFePO_4$/C nanofibers are weakened or partly broken by the adhesion of phosphorus, thereby improving the electrochemical performance of $LiFePO_4$/C nanofibers. We suggest that tailoring the surface bonding structure of $LiFePO_4$/C nanofibers by phosphorus incorporation can enhance the kinetics of Li ion migration through the thick carbon layers coated on the surface of $LiFePO_4$/C. Herein, our aim was to elucidate the effects of phosphorus treatment on the surface bonding structure and electrochemical performance of $LiFePO_4$/C nanofibers prepared by the electrospinning method.

EXPERIMENTAL SECTION

Materials. Lithium hydroxide monohydrate ($LiOH{\cdot}H_2O$, 98%, Samchun Chemicals), iron(II) sulfate heptahydrate ($FeSO_4{\cdot}7H_2O$, 99%, Kanto Chemical), phosphoric acid (H_3PO_4, 85%, Aldrich), citric acid anhydrous ($C_6H_8O_7$, 99.5%, Junsei), and PVP (C_6H_9NOx, M_w: 1,300,000) were purchased and used without further purification.

Preparation of $LiFePO_4$/C Nanofibers by Electrospinning. To prepare the electrospinning solution, 0.6 mM/mL of lithium hydroxide monohydrate, iron(II) sulfate heptahydrate, and phosphoric acid (stoichiometric ratio of Li/Fe/P to 1:1:1) were dissolved in deionized water. Then, 36 mg/mL of citric acid and 16 wt % of polyvinylpyrrolidone were mixed with the prepared solution, and it was vigorously stirred for 3 h. The homogeneously mixed solution was immediately loaded into a plastic syringe equipped with a 23-gauge needle. The needle was connected to a high voltage supply (DC voltage of 17 kV). The feeding rate for the precursor solution was 0.2 mL/h, and the distance between the needle and a collector was 8 cm. The electrospinning process was conducted in air. After spinning, the collected nanofibers were dried in a vacuum oven overnight. The electrospun nanofibers were calcined in a tube furnace at 750 °C at the rate of 100 °C/h for 10 h in a mixed gas flow of 5 wt % H_2 + Ar.

Preparation of Phosphidated $LiFePO_4$/C Nanofibers. The electrospun $LiFePO_4$/C nanofibers (0.01 g) and TOP (100 μL) were mixed in a mortar under an Ar atmosphere. The resulting black powder was loaded into a quartz boat reactor, and the reactor was placed in the middle of a tube furnace. After stabilizing the gas flow (Ar/H_2, 5 wt %) system for 30 min, the temperature of the furnace was increased from room temperature to 600 °C, with the heating rate of 4 °C/min, and then maintained at 600 °C for 2 h.

Characterization. The morphologies of the $LiFePO_4$/C nanofibers were characterized by scanning electron microscopy (SEM) and high resolution-transmission electron microscopy (HR-TEM) (JEOL JSM-6700F). The crystal structures of the $LiFePO_4$/C nanofibers were confirmed by X-ray powder diffraction (XRD) (Bruker Miller Co. D8-

Advance, Cu Kα radiations), and their average lattice parameters were determined by iterative least-squares refinements for their XRD patterns. The surface binding energy of the materials was verified by X-ray photoelectron spectroscopy (XPS) (Thermo Fisher Scientific Co. theta probe base system). The following binding energies were referenced: for P 2p (P−O bond, 132.7 eV), C 1s (C−C bond, 284.6 eV; C−O bond, 286.4 eV; C═O bond, 289.07 eV), and O 1s (C−O bond, 533.5 eV; C═O bond, 531.6 eV; P−O−P bond, 533.1 eV; P_2O_5 bond, 534.3 eV) spectra. The residual carbon content in the products was determined by thermogravimetric analysis (TGA), and their average pore sizes were calculated from Barret−Joyner−Halenda (BJH) plots.

Electrochemical Measurements. Electrodes were fabricated by mixing each active material ($LiFePO_4$/C nanofibers), ketjen black, acetylene black, and polyvinylidene fluoride with a weight ratio of 60:20(6:4):20 using *N*-methylpyrrolidone as a solvent. The resulting slurries were pasted onto Al foils and then dried in a vacuum oven at 120 °C for 5 h. After drying, the electrode foils were pressed and then punched into a disk type with a diameter of 1.3 cm. The electrochemical properties of the electrodes were evaluated using CR2032 coin-type cells assembled in an argon-filled glovebox. Li metal foil was used as a counter electrode, and 1 M solution of $LiPF_6$ in ethylene carbonate and dimethyl carbonate (1:1, v/v) was employed as an electrolyte. The prepared cells were charged and discharged galvanostatically between 2.5 and 4.3 V (vs Li^+/Li) at room temperature. Open circuit voltage (OCV) and closed circuit voltage (CCV) tests were performed to investigate the change in the electrode resistance during the initial Li ion insertion/extraction. The two electrode cells activated for the first two cycles were subjected to electrochemical impedance spectroscopy (EIS) with a sinusoidal voltage signal (5 mV) over a frequency range from 1000 kHz to 100 mHz.

RESULTS AND DISCUSSION

Phosphidated $LiFePO_4$/C nanofibers were prepared by the thermal treatment of a $LiFePO_4$/C nanofiber-TOP mixture in a tube furnace (see details in the Experimental Section). TOP is a widely known surfactant that can serve as both a stabilizing ligand and a phosphorus source.

The SEM images of pristine and phosphidated $LiFePO_4$/C nanofibers are shown in Figure 2a,b, respectively. As observed in Figure 2a, long and continuous $LiFePO_4$/C nanofibers were obtained from electrospun $LiFePO_4$ polyvinylpyrrolidone (PVP) nanofiber precursors (Figure S1, Supporting Information) after calcination at 750 °C for 10 h in a mixed gas flow of 5 wt % H_2 + Ar. The homogeneous $LiFePO_4$/C nanofibers with a diameter of ∼100 nm were randomly oriented, and they formed an interconnected fiber network. As confirmed in Figure 2b, the pristine $LiFePO_4$/C nanofibers maintained a well-fabricated 1D morphology even after phosphidation. Figure 2c,d shows low-resolution TEM images of the pristine and phosphidated $LiFePO_4$/C nanofibers commonly coated by amorphous carbon layers with 10−20 nm in thickness. The residual carbon content in these nanofibers, estimated by TGA, was approximately 25 wt %, in agreement with the thick carbon coating layers on the surface of both nanofibers (Figure S2, Supporting Information). The high-resolution TEM images and corresponding selected area diffraction pattern (SADP) of the pristine and phosphidated $LiFePO_4$ nanofibers revealed that a single-crystalline $LiFePO_4$ phase formed inside the $LiFePO_4$/C nanofibers (Figure 2e,f). The lattice spacing of the pristine $LiFePO_4$/C nanofibers was 0.30 nm, corresponding to (020) lattice planes of the $LiFePO_4$, while the phosphidated $LiFePO_4$/C nanofibers showed (111) lattice planes, with the lattice spacing of 0.35 nm.

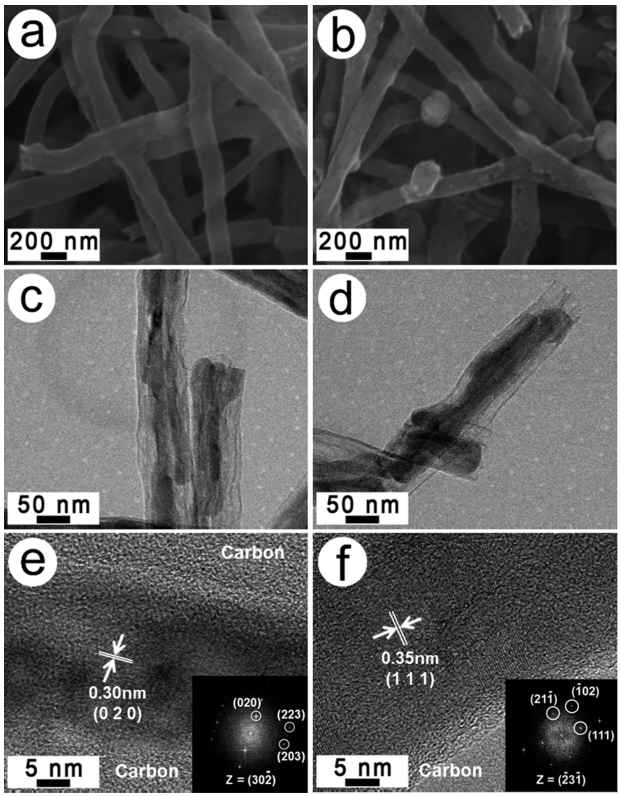

Figure 2. Scanning electron microscopy images of (a) pristine and (b) phosphidated $LiFePO_4$/C nanofibers. Low-resolution and high-resolution transmission electron microscopy images of the (c, e) pristine and (d, f) phosphidated $LiFePO_4$/C nanofibers, along with the corresponding selected area diffraction pattern.

Figure 3 shows the XRD patterns of the pristine and phosphidated $LiFePO_4$/C nanofibers. The XRD pattern

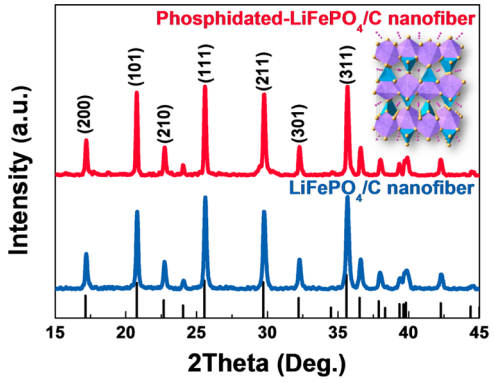

Figure 3. X-ray diffraction patterns of pristine and phosphidated $LiFePO_4$/C nanofibers.

acquired from the pristine $LiFePO_4$/C nanofibers was found to be in agreement with the reference patterns of $LiFePO_4$, with an ordered olivine structure (space group: *Pnma*).[20,22,36−38] In addition, a minor difference between the pristine and phosphidated $LiFePO_4$/C nanofibers was observed in their XRD patterns including lattice parameter (Table S1, Supporting Information). The unchanged bulk structure, morphology, and carbon content of the $LiFePO_4$/C nanofibers after phosphidation convinced us that the incorporated phosphorus ions primarily influenced the surface properties of the

dx.doi.org/10.1021/am5018122 | ACS Appl. Mater. Interfaces 2014, 6, 9435−9441

$LiFePO_4$/C nanofibers (Figures 2 and S2, Supporting Information).

The XPS valence band spectra of the pristine and phosphidated $LiFePO_4$/C nanofibers are shown in Figure 4.

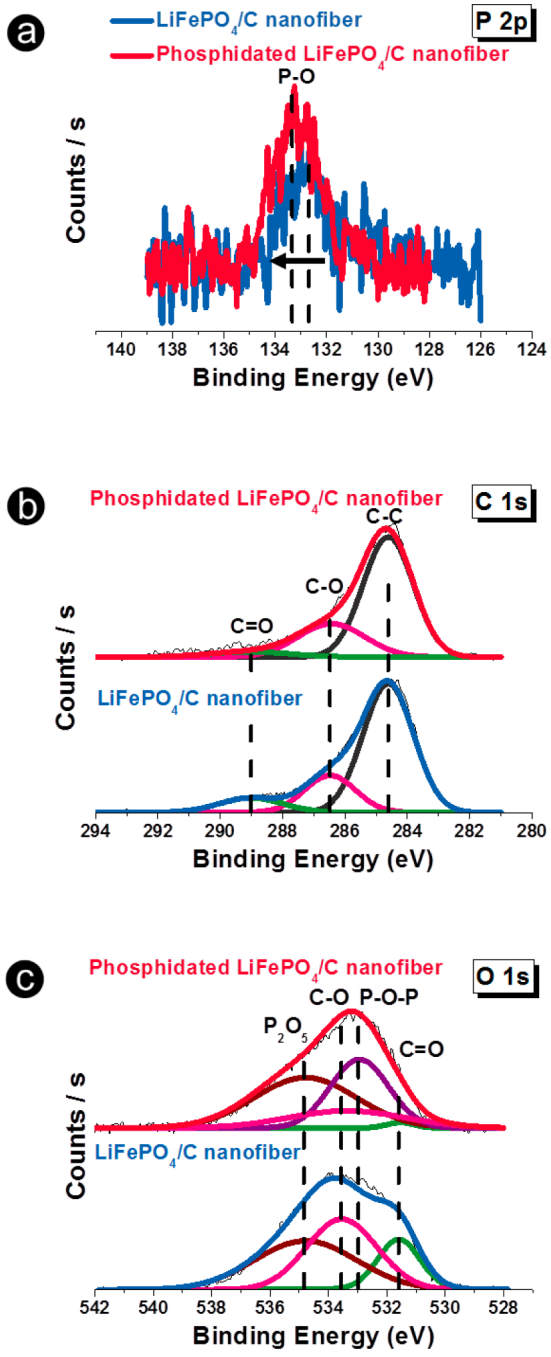

Figure 4. (a) P 2p, (b) C 1s, and (c) O 1s X-ray photoelectron spectroscopy core peaks for pristine and phosphidated $LiFePO_4$/C nanofibers.

XPS is an appropriate tool for determining the chemical states on the surface of materials. From the P 2p spectra of the $LiFePO_4$/C nanofibers in Figure 4a, we confirmed that the P 2p XPS core peak was shifted to the left and that the intensity of the P−O bonds increased as a result of phosphidation indicating that the electrons in the P 2p core level of the phosphidated $LiFePO_4$/C nanofibers (133.4 eV) have a higher binding energy than those of the pristine $LiFePO_4$/C (132.7 eV). The increase in the binding energy and intensity of the P−O bonds on the surface of the $LiFePO_4$/C nanofibers might be attributed to the adsorption of phosphorus onto the P−O dangling bonds on the surface of the $LiFePO_4$ nanofibers, which resultantly reinforces the P−O bonds or PO_4 polyhedra. The deconvoluted C 1s spectra of the $LiFePO_4$/C nanofibers were identified as C−O (286.4 eV), C═O (289.1 eV), and C−C (284.6 eV) bonds, as described in Figure 4b. The intensities of the C−O and C═O bonds of the phosphidated $LiFePO_4$/C were lower than those of the pristine $LiFePO_4$/C nanofibers. As shown in Figure 4c, the O1 region also reflected this tendency that C−O and C═O bonds are weakened along with the evolution of P−O−P bonds. The new formation of P−O−P bonds proves that phosphorus was directly bonded to the P−O dangling bonds, implying that the existing strong C═O bonds were broken by the adhesion of phosphorus on the surface of the $LiFePO_4$ nanofibers and the carbon webs around them could probably be reduced after phosphidation. In addition, the average pore size inside the nanofibers was augmented according to the calculation results from the BJH plots (Table S2, Supporting Information). We believe that, when the phosphorus ions penetrate the carbon webs, the empty space between the adjacent carbon webs could be enlarged by phosphorus diffusion to the surface of the $LiFePO_4$ nanofibers.

Figure 5a shows the initial galvanostatic voltage profiles (0.1 C-rate, 1 C = 170 mAh g^{-1}) of the pristine and phosphidated $LiFePO_4$/C nanofibers. Although the $LiFePO_4$/C nanofibers have a well-fabricated 1D nanostructure, the discharge capacity of the pristine $LiFePO_4$/C is ∼127 mA h g^{-1}, which is much lower than the theoretical discharge capacity (∼170 mA h g^{-1}) of $LiFePO_4$. Meanwhile, the phosphidated $LiFePO_4$/C nanofibers displayed a high discharge capacity of ∼163 mA h g^{-1}, with low-voltage polarization during the first cycle. The dQ/dV vs the voltage plots of the $LiFePO_4$/C nanofibers are given to compare their electrochemical reactions and kinetics in Figure 5b. A pair of sharp peaks around 3.45 V demonstrated that only one reversible electrochemical reaction corresponding to the voltage plateau of a Fe^{3+}/Fe^{2+} redox couple occurred in the $LiFePO_4$/C nanofibers. Therein, the peak potential difference between charge and discharge was remarkably reduced by the incorporation of phosphorus into the surface of the $LiFePO_4$/C nanofibers. This finding shows significant agreement with the results obtained from their initial charge−discharge profiles (Figure 5a).

The rate capabilities of the pristine and phosphidated $LiFePO_4$/C nanofibers are presented in Figure 5c. The discharge capacity of the $LiFePO_4$/C nanofibers achieved at low current densities (0.2 and 0.5 C) was similar to that measured at 0.1 C, but a gradual decrease in the discharge capacity was observed as the applied current density increased (>0.5 C). However, unlike the pristine $LiFePO_4$/C nanofibers, the $LiFePO_4$/C treated by phosphorus featured a high discharge capacity of ∼87 mA h g^{-1}, even at a high current density of 20 C. This result implies that Li ion movement into/out of the $LiFePO_4$/C nanofibers became kinetically more favorable after phosphidation. Considering that the $LiFePO_4$/C nanofibers were consistent in bulk crystal structure, morphology, and carbon content irrespective of phosphidation, the enhancement in the rate capability of the phosphidated samples and their increased initial discharge capacity compared to the pristine ones may be due to variation in their surface properties induced by phosphorus incorporation. As previously discussed

dx.doi.org/10.1021/am5018122 | ACS Appl. Mater. Interfaces 2014, 6, 9435−9441

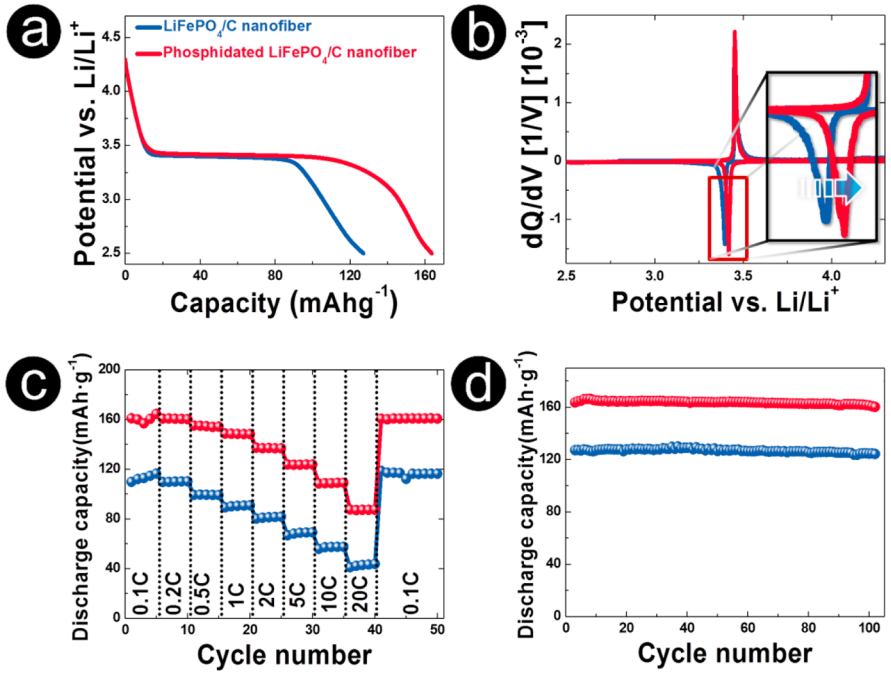

Figure 5. (a) Initial galvanostatic (0.1 C-rate, 1 C = 170 mAh g^{-1}) voltage profiles, (b) dQ/dV vs voltage plots for the 1st cycle, (c) cycling performance (0.1 C), and (d) rate capability of the pristine and phosphidated $LiFePO_4$/C nanofibers.

in the XPS results, strong interactions between carbon and oxygen atoms on the surface of the $LiFePO_4$ nanofibers are weakened or partly broken by the adhesion of phosphorus. This facilitates Li ion transport through the electrode/electrolyte interface by forming noble Li conducting pathways along the reduced carbon web by phosphorus.

We compared the cycling performances of the pristine and phosphidated $LiFePO_4$/C nanofibers at 0.1 C as shown in Figure 5d. Both types of nanofibers featured good cycling performance, but after 100 cycles, the pristine $LiFePO_4$/C exhibited a discharge capacity of ~124 mA h g^{-1}, corresponding to ~97.6% of its initial discharge capacity (~127 mA h g^{-1}), whereas the phosphidated $LiFePO_4$/C showed a high discharge capacity of ~160 mA h g^{-1}, corresponding to ~98.2% of its initial discharge capacity (~163 mA h g^{-1}). The superior cycling performance of the $LiFePO_4$ nanofibers embedded in a large amount of amorphous carbon is partly due to the improved structural stability of the $LiFePO_4$ lattice structure. The improvement in the structural stability was induced by the accommodation of stress/strain within the $LiFePO_4$ nanofibers during cycling and the reduced reaction area exposed to the electrolyte by surrounding inactive carbons.[39,40] Tailoring the surface bonding structure of the $LiFePO_4$/C nanofibers by phosphorus incorporation might improve the structural stability of $LiFePO_4$/C because the polyanion tetrahedra (PO_4) in $LiFePO_4$ crystals could be stabilized more by the reinforcement of the P−O bonds on their surface, as explained in Figure 4a.

Figure 6a represents the electrode resistance of the pristine and phosphidated $LiFePO_4$/C nanofibers as a function of the state of charge. The electrode resistance was estimated from their OCV and CCV profiles (Figure S3, Supporting Information). It has been reported that the electrode resistance is correlated with the polarization (ΔV) by Ohm's law ($R = \Delta V/I$). Because the overall electrode resistance of the phosphidated $LiFePO_4$/C was lower than that of the pristine $LiFePO_4$/C nanofibers, we could believe that the increased

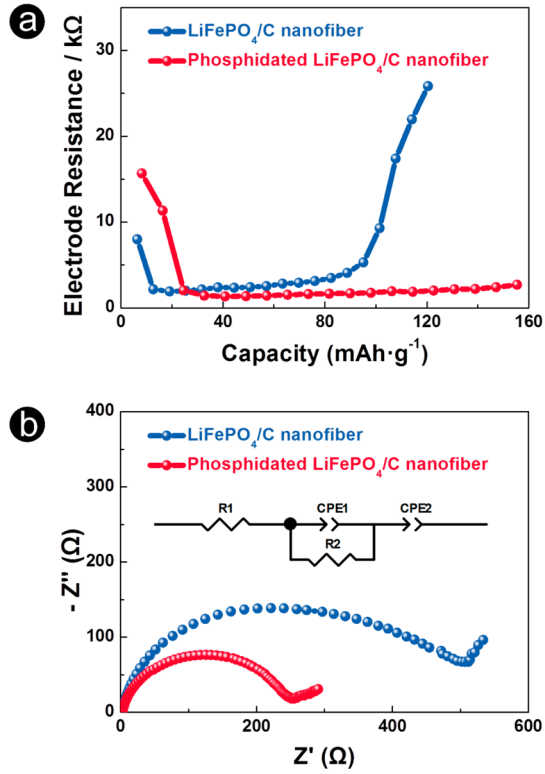

Figure 6. (a) Overall electrode resistance estimated from the OCV/CCV profiles; (b) Nyquist plots of pristine and phosphidated $LiFePO_4$/C nanofibers.

discharge capacity and the improved kinetic properties of the $LiFePO_4$/C nanofibers through phosphidation are closely associated with the electrode resistance change of the $LiFePO_4$/C nanofibers. When ignoring insignificant discrepancies during electrode and cell preparation, electrode resistance can be considered as a characteristic of the materials.

dx.doi.org/10.1021/am5018122 | ACS Appl. Mater. Interfaces 2014, 6, 9435−9441

The EIS spectra of the $LiFePO_4$/C nanofibers measured after cell formation for the first two cycles showed a significant reduction in their charge transfer resistance at the electrode/electrolyte interface by phosphidation (Figure 6b). In the EIS spectra, the charge transfer resistance determined from a semicircle in the high-middle frequency region is attributed to mixed Li ionic and electronic conduction through the interfaces. Taking the slight difference in the amount of conductive carbon between the two types of $LiFePO_4$/C nanofibers into account, the reduced electrode and charge transfer resistance of the $LiFePO_4$/C nanofibers by phosphidation resulted from facile Li ion migration through electrode/electrolyte interface. This idea is supported by the results of the XPS analyses and the electrochemical test for the pristine and phosphidated $LiFePO_4$/C nanofibers (Figures 4 and 5). Therefore, the phosphidation method proposed in the present study is an effective approach for tailoring the surface structure of electrode materials to improve their kinetics. Moreover, our finding of high Li ion transport induced by phosphidation can be widely applied to any other carbon-coated electrode materials.

CONCLUSIONS

In summary, we succeeded in tailoring the chemical bonding structure on the surface of $LiFePO_4$/C nanofibers by phosphidation. Pristine $LiFePO_4$/C nanofibers prepared by the electrospinning method consisted of 1D $LiFePO_4$ nanofibers and thick carbon coating layers. Despite the numerous merits of the 1D nanostructured $LiFePO_4$, the migration of Li ions into/out of the nanofibers is hindered by the dense and thick carbon layers that form on the surfaces of the $LiFePO_4$ nanofibers. These prevent not only the penetration of the electrolyte into the inner $LiFePO_4$ nanofibers but also facile Li ion transport at the electrode/electrolyte interface. The phosphidated $LiFePO_4$/C nanofibers obtained by thermal decomposition of TOP showed a high initial discharge capacity (~163 mA h g^{-1}), greatly improved rate capability (~87 mA h g^{-1} at a current density of 20 C), and excellent cycling performance (~98.2% of its initial discharge capacity after 100 cycles), although the pristine and phosphidated $LiFePO_4$/C nanofibers had similar bulk crystal structure, morphology, and carbon content. We found that the enhanced electrochemical performance of the $LiFePO_4$/C nanofibers induced by the incorporation of phosphorus contributed to the formation of noble Li ion conducting pathways built along the reduced carbon webs by phosphorus. The existing strong interactions between carbon and oxygen atoms on the surface of the pristine $LiFePO_4$/C nanofibers were weakened or partly broken by the adhesion of phosphorus. This improved the kinetics of Li ion migration through the thick carbon layers on the surfaces of the $LiFePO_4$ nanofibers.

ASSOCIATED CONTENT

Supporting Information

Experimental details, characterization, and analysis of data. This material is available free of charge via the Internet at http://pubs.acs.org.

AUTHOR INFORMATION

Corresponding Author

*Phone: +82 2 2260 8674. Fax: +82 2 2268 8550. E-mail: dake1234@dongguk.edu.

Author Contributions

‡Y.C.L. and D.-W.H. contributed equally.

Notes

The authors declare no competing financial interest.

ACKNOWLEDGMENTS

This research was supported by (NRF-2010-C1AAA001-0029018) and the Basic Science Research Program (S-2013-A0434-00024) through the National Research Foundation of Korea funded by the Ministry of Education.

REFERENCES

(1) Joachin, H.; Kaun, T. D.; Zaghib, K.; Prakash, J. Electrochemical and thermal studies of carbon-coated $LiFePO_4$ cathode. *J. Electrochem. Soc.* **2009**, *156*, A401−A406.

(2) Maccario, M.; Croquennec, L.; Cras, F. L.; Delmas, C. Electrochemical performances in temperature for a C-containing $LiFePO_4$ composite synthesized at high temperature. *J. Power Sources* **2008**, *183*, 411−417.

(3) Yang, M. R.; Ke, W. H.; Wu, S. H. Preparation of $LiFePO_4$ powders by co-precipitation. *J. Power Sources* **2005**, *146*, 539−543.

(4) Wu, X. L.; Jiang, L. Y.; Cao, F. F.; Guo, Y. G.; Wan, L. J. $LiFePO_4$ nanoparticles embedded in a nanoporous carbon matrix: Superior cathode material for electrochemical energy-storage devices. *Adv. Mater.* **2009**, *21*, 2710−2714.

(5) Dominko, R.; Bele, M.; Goupil, J. M.; Gaberscek, M.; Hanzel, D.; Arcon, I.; Jamnik, J. Wired porous cathode materials: A novel concept for synthesis of $LiFePO_4$. *J. Chem. Mater.* **2007**, *19*, 2960−2969.

(6) Wang, Y.; Wang, Y.; Hosono, E.; Wang, K.; Zhou, H. The design of a $LiFePO_4$/carbon nanocomposite with a core−shell structure and its synthesis by an in situ polymerization restriction method. *Angew. Chem.* **2008**, *120*, 7571−7575.

(7) Xie, H. M.; Wang, R. S.; Ying, J. R.; Zhang, L. Y.; Jalbout, A. F.; Yu, H. Y.; Yang, G. L.; Pan, X. M.; Su, Z. M. Optimized $LiFePO_4$−polyacene cathode material for lithium-ion batteries. *Adv. Mater.* **2006**, *18*, 2609−2613.

(8) Yang, S.; Song, Y.; Zavalij, P. Y.; Whittingham, M. S. Reactivity, stability and electrochemical behavior of lithium iron phosphates. *Electrochem. Commun.* **2002**, *4*, 239−244.

(9) Amin, R.; Balaya, P.; Maier, J. Anisotropy of electronic and ionic transport in LiFePO4 single crystals. *Electrochem. Solid-State Lett.* **2007**, *10*, A13−A16.

(10) Morgan, D.; Van der Ven, A.; Ceder, G. Li conductivity in Li_xMPO_4 (M = Mn, Fe, Co, Ni) olivine materials. *Electrochem. Solid-State Lett.* **2004**, *7*, A30−A32.

(11) Prosini, P. P.; Lisi, M.; Zane, D.; Pasquali, M. Determination of the chemical diffusion coefficient of lithium in $LiFePO_4$. *Solid State Ionics* **2002**, *148*, 45−51.

(12) Delacourt, C.; Laffont, L.; Bouchet, R.; Wurm, C.; Leriche, J. B.; Morcrette, M.; Tarascon, J. M.; Masquelier, C. Toward understanding of electrical limitations (electronic, ionic) in $LiMPO_4$ (M = Fe, Mn) electrode materials. *J. Electrochem. Soc.* **2005**, *152*, A913−A921.

(13) Arico, A. S.; Bruce, P. G.; Scrosati, B.; Tarascon, J. M. Nanostructured materials for advanced energy conversion and storage devices. *Nat. Mater.* **2005**, *4*, 366−377.

(14) Manthiram, A.; Vadivel Murugan, A.; Sarkar, A.; Muraliganth, T. Nanostructured electrode materials for electrochemical energy storage and conversion. *Energy Environ. Sci.* **2008**, *1*, 621−638.

(15) Delacourt, C.; Poizot, P.; Levasseur, S.; Maquelier, C. Size effects on carbon-free $LiFePO_4$ powders the key to superior energy density. *Electrochem. Solid-State Lett.* **2006**, *9*, A352−A355.

(16) Hsu, K. F.; Tsay, S. Y.; Hwang, B. J. Synthesis and characterization of nano-sized $LiFePO_4$ cathode materials prepared by a citric acid-based sol−gel route. *J. Mater. Chem.* **2004**, *14*, 2690−2695.

(17) Wang, Y.; Li, H.; He, P.; Hosono, E.; Zhou, H. Nano active materials for lithium-ion batteries. *Nanoscale* **2010**, *2*, 1294−1305.

(18) Wang, Y.; Wang, Y.; Hosono, E.; Wang, K.; Zhou, H. The design of a $LiFePO_4$/carbon nanocomposite with a core−shell structure and its synthesis by an in situ polymerization restriction method. *Angew. Chem., Int. Ed.* **2008**, *47*, 7461−7465.
(19) Oh, S. W.; Myung, S. T.; Oh, S. M.; Oh, K. H.; Amine, K.; Scrosati, B.; Sun, Y. K. Double carbon coating of $LiFePO_4$ as high rate electrode for rechargeable lithium batteries. *Adv. Mater.* **2010**, *22*, 4842−4845.
(20) Dong, Y. Z.; Zhao, Y. M.; Chen, Y. H.; He, Z. F.; Kuang, Q. Optimized carbon-coated $LiFePO_4$ cathode material for lithium-ion batteries. *Mater. Chem. Phys.* **2009**, *115*, 245−250.
(21) Chen, Z.; Dahn, J. R. Reducing carbon in $LiFePO_4$/C composite electrodes to maximize specific energy, volumetric energy, and tap density. *J. Electrochem. Soc.* **2002**, *149*, A1184−A1189.
(22) Wang, G.; Shen, X.; Yao, J. One-dimensional nanostructures as electrode materials for lithium-ion batteries with improved electrochemical performance. *J. Power Sources* **2009**, *189*, 543−546.
(23) Saji, V. S.; Kim, Y. S.; Kim, T. H.; Cho, J. P.; Song, H. K. One-dimensional (1D) nanostructured and nanocomposited $LiFePO_4$: Its perspective advantages for cathode materials of lithium ion batteries. *Phys. Chem. Chem. Phys.* **2011**, *13*, 19226−19237.
(24) Wang, Y.; Cao, G. Developments in nanostructured cathode materials for high-performance lithium-ion batteries. *Adv. Mater.* **2008**, *20*, 2251−2269.
(25) Cho, Y. D.; Fey, G. T. K.; Kao, H. M. The effect of carbon coating thickness on the capacity of $LiFePO_4$/C composite cathodes. *J. Power Sources* **2009**, *189*, 256−262.
(26) Dominko, R.; Bele, M.; Gaberscek, M.; Remskar, M.; Hanzel, D.; Pejovnik, S.; Jamnik, J. Impact of the carbon coating thickness on the electrochemical performance of $LiFePO_4$/C composites. *J. Electrochem. Soc.* **2005**, *152*, A607−A610.
(27) Zhao, S. X.; Ding, H.; Wang, Y. C.; Li, B. H.; Nan, C. W. Improving rate performance of $LiFePO_4$ cathode materials by hybrid coating of nano-Li_3PO_4 and carbon. *J. Alloys Compd.* **2013**, *566*, 206−211.
(28) Lee, S. H.; Jung, M. J.; Im, J. S.; Sheem, K. Y.; Lee, Y. S. Preparation and characterization of electrospun $LiFePO_4$/carbon complex improving rate performance at high C-rate. *Res. Chem. Intermed.* **2010**, *36*, 591−602.
(29) Hagen, R.; Lorrmann, H.; Möller, K. C.; Mathur, S. Electrospun $LiFe_{1-y}Mn_yPO_4$/C nanofiber composites as self-supporting cathodes in Li-ion batteries. *Adv. Energy Mater.* **2012**, *2*, 553−559.
(30) Toprakci, O.; Ji, L.; Lin, Z.; Toprakci, H. A.K.; Zhang, X. Fabrication and electrochemical characteristics of electrospun $LiFePO_4$/carbon composite fibers for lithium-ion batteries. *J. Power Sources* **2011**, *196*, 7692−7699.
(31) Choi, C. H.; Park, S. H.; Woo, S. I. Phosphorus−nitrogen dual doped carbon as an effective catalyst for oxygen reduction reaction in acidic media: Effects of the amount of P-doping on the physical and electrochemical properties of carbon. *J. Mater. Chem.* **2012**, *22*, 12107−12115.
(32) Kim, M. J.; Yeon, J. T.; Hong, K.; Lee, S. I.; Choi, N. S.; Kim, S. S. Effects of phosphorous-doping on electrochemical performance and surface chemistry of soft carbon electrodes. *Bull. Korean Chem. Soc.* **2013**, *34*, 2029−2035.
(33) Molina-Sabio, M.; Rodriguez-Reinoso, F.; Caturla, F.; Selles, M. J. Development of porosity in combined phosphoric acid-carbon dioxide activation. *Carbon* **1996**, *34*, 457−462.
(34) Larrude, D. G.; Maia da Costa, M. E. H.; Monteiro, F. H.; Pinto, A. L.; Freire, F. L., Jr Characterization of phosphorus-doped multiwalled carbon nanotubes. *J. Appl. Phys.* **2012**, *111*, 064315.
(35) Wu, Y.; Fang, S.; Jiang, Y. Carbon anodes for a lithium secondary battery based on polyacrylonitrile. *J. Power Sources* **1998**, *75*, 201−206.
(36) Piana, M.; Arrabito, M.; Bodoardo, S.; D'Epifanio, A.; Satolli, D.; Croce, F.; Scrosati, B. Characterization of phospho-olivines as materials for Li-ion cell cathodes. *Ionics* **2002**, *8*, 17−26.
(37) Moreau, P.; Guyomard, D.; Gaubicher, J.; Boucher, F. Structure and stability of sodium intercalated phases in olivine $FePO_4$. *Chem. Mater.* **2010**, *22*, 4126−4128.
(38) Chung, S. Y.; Bloking, J. T.; Chiang, Y. M. Electronically conductive phospho-olivines as lithium storage electrodes. *Nat. Mater.* **2002**, *1*, 123−128.
(39) Gabrisch, H.; Wilcox, J.; Doeff, M. TEM studies of carbon coated $LiFePO_4$ after charge discharge cycling. *ECS Trans.* **2007**, *3*, 29−36.
(40) Kim, H. S.; Chung, Y. H.; Kang, S. H.; Sung, Y. E. Electrochemical behavior of carbon-coated SnS_2 for use as the anode in lithium-ion batteries. *Electrochim. Acta* **2009**, *54*, 3606−3610.